Supplementary Information

Hydrogel-stabilized supercooled salt hydrates for seasonal storage and controlled release of solar-thermal energy

Yizhe Liu[a, b], *Xiaoxiang Li*[a], *Yangzhe Xu*[a], *Benwei Fu*[a, c], *Chengyi Song*[a, c], *Wen Shang*[a], *Peng Tao*[a, c, *], *Tao Deng*[a, c, *]

[a]State Key Laboratory of Metal Matrix Composites, School of Materials Science and Engineering, Shanghai Jiao Tong University, 800 Dong Chuan Road, Shanghai 200240, China

[b]Materials Genome Initiative Center, School of Materials Science and Engineering, Shanghai Jiao Tong University, 800 Dong Chuan Road, Shanghai 200240, China

[c]National Engineering Research Center of Special Equipment and Power System for Ship and Marine Engineering, Shanghai 200030, China

*Email: taopeng@sjtu.edu.cn (Peng Tao), dengtao@sjtu.edu.cn (Tao Deng)

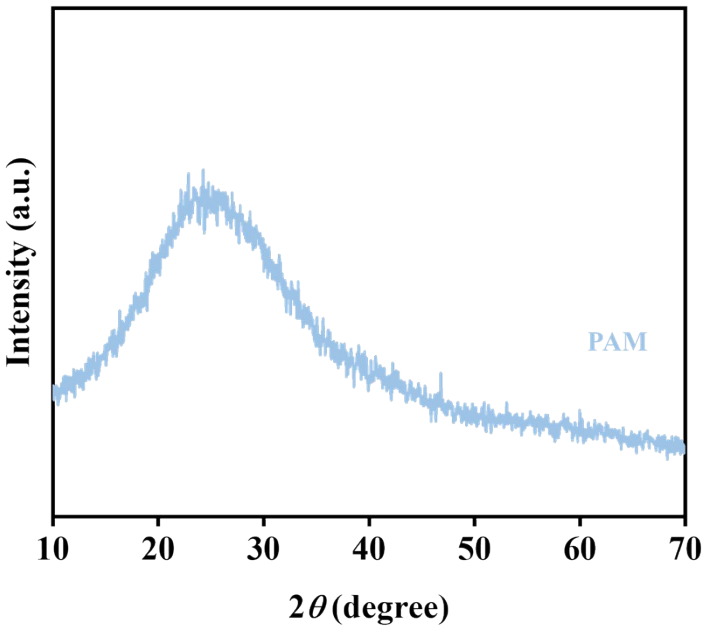

Figure S1 XRD pattern of PAM hydrogel

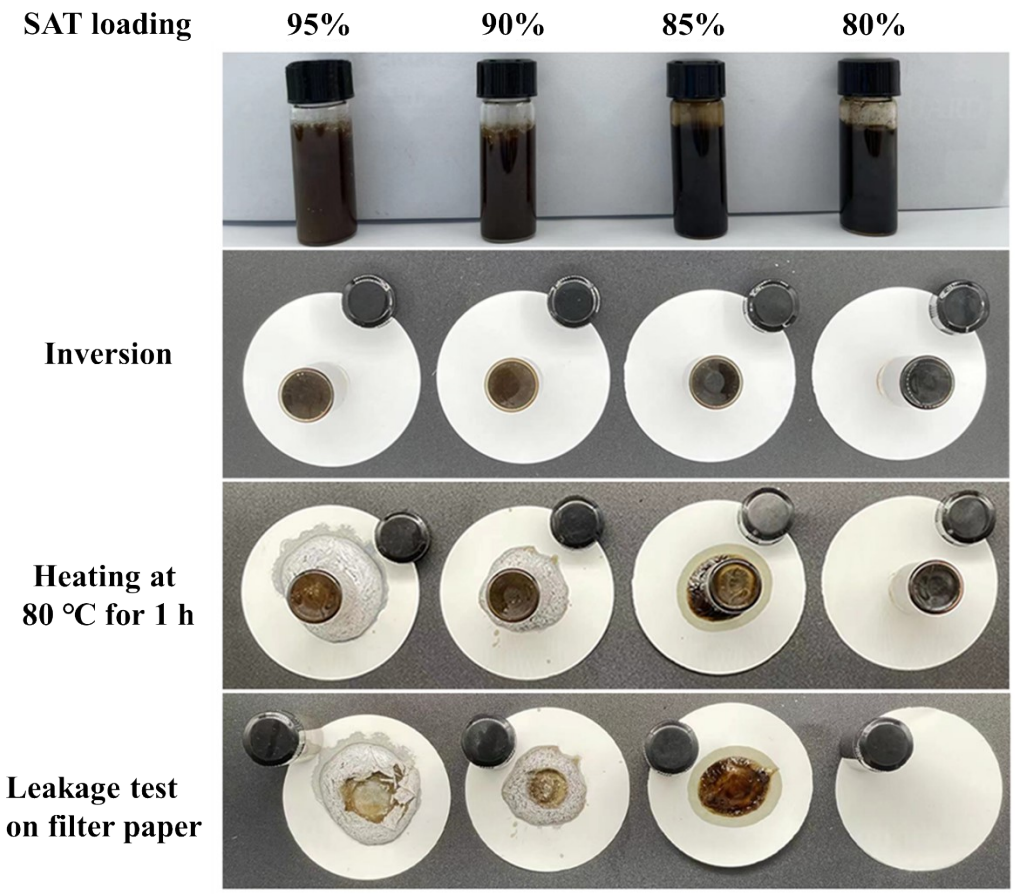

Figure S2 Photos showing anti-leaking performances of SPP composites loaded with different concentration of SAT (80 wt%, 85 wt%, 90 wt%, 95 wt%).

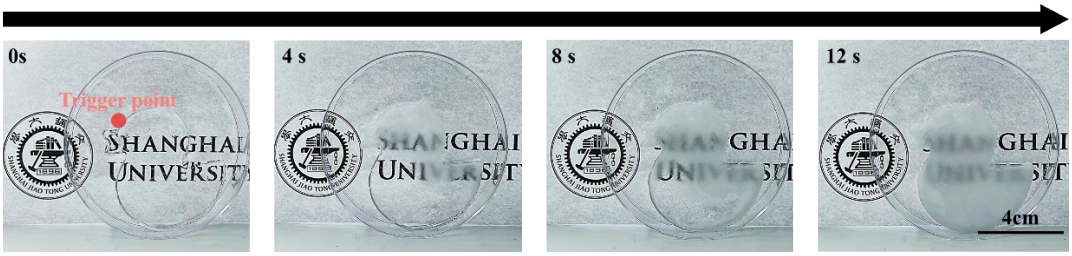

Figure S3 Time-sequential photographs showing triggered crystallization of supercooled SAT-PAM composites.

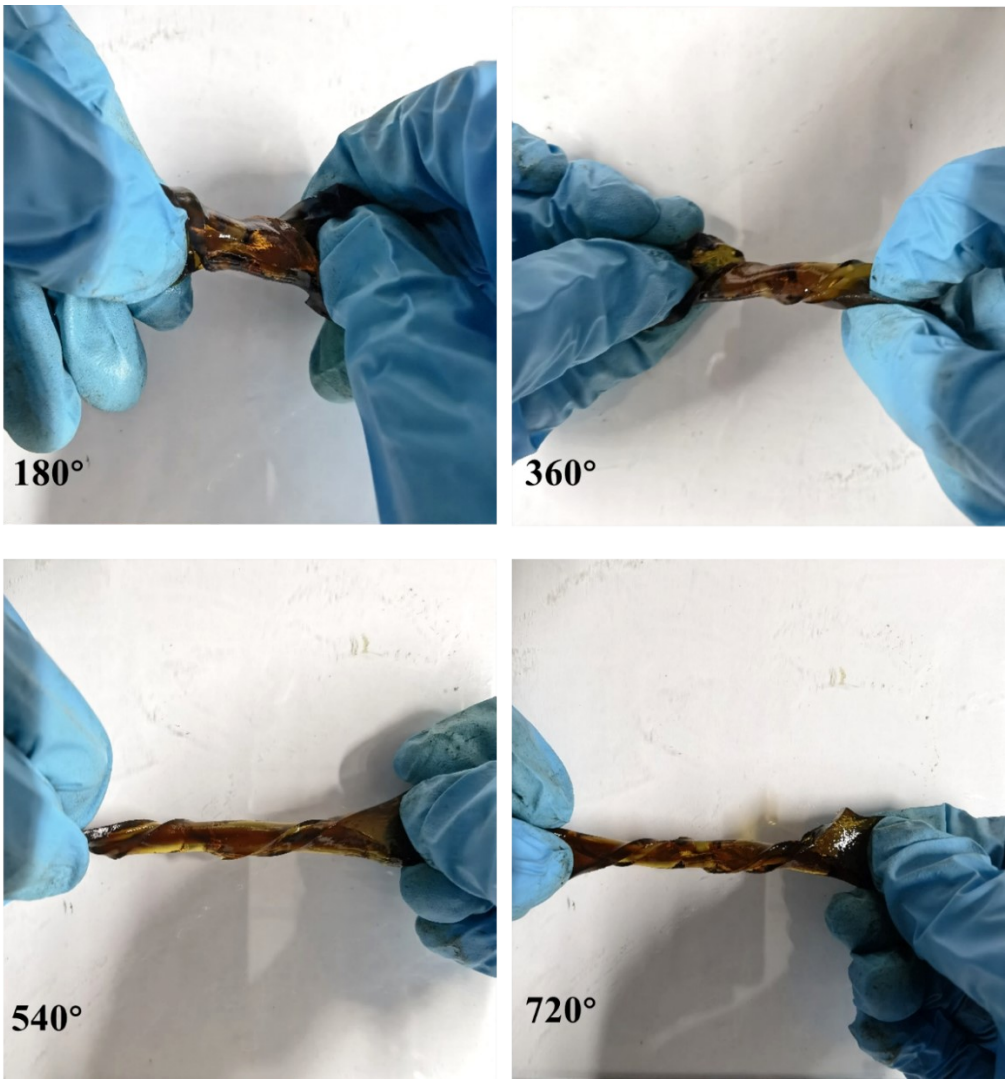

Figure S4 Photos showing continuous twisting behavior of SPP composites.

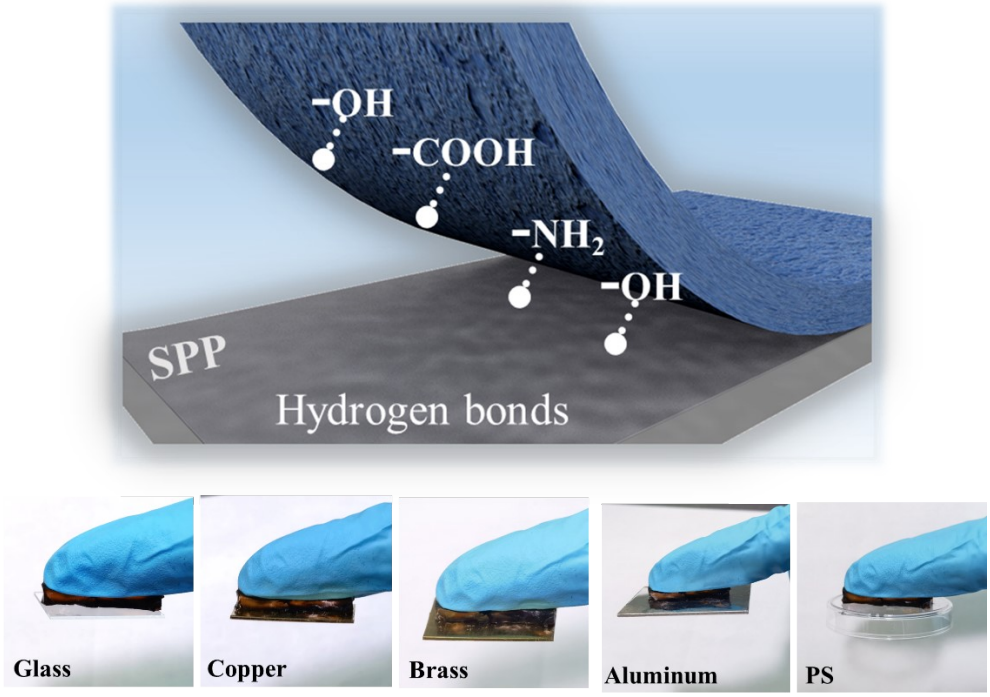

Figure S5 Robust self-adhesion of SPP composites with different types of substrates (glass, copper, brass, aluminum, polystyrene petri dish).

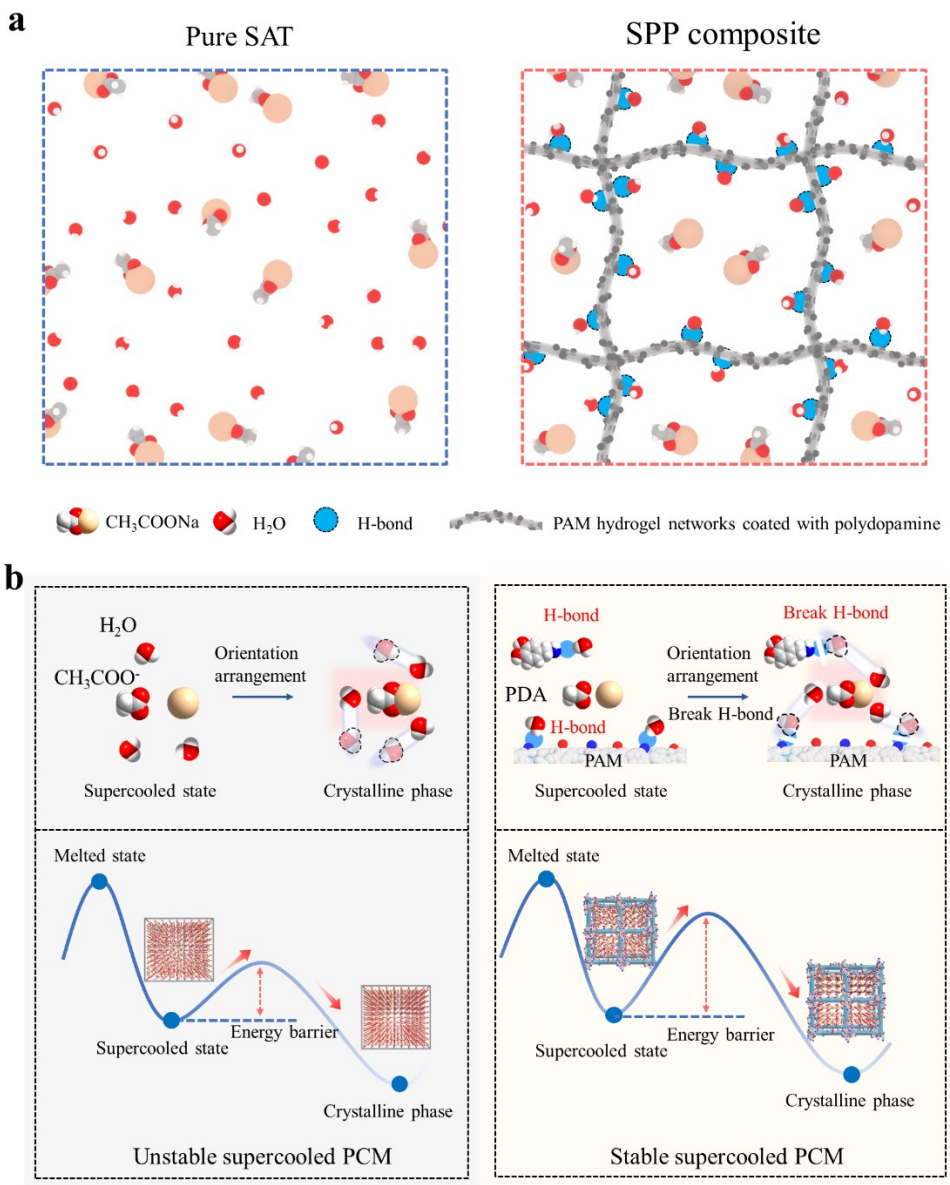

Figure S6 (a) Schematic comparing intermolecular interaction in neat SAT and SPP composites. (b) Schematic showing unstable supercooling of neat SAT and stable supercooling of SAT within PSS composites.

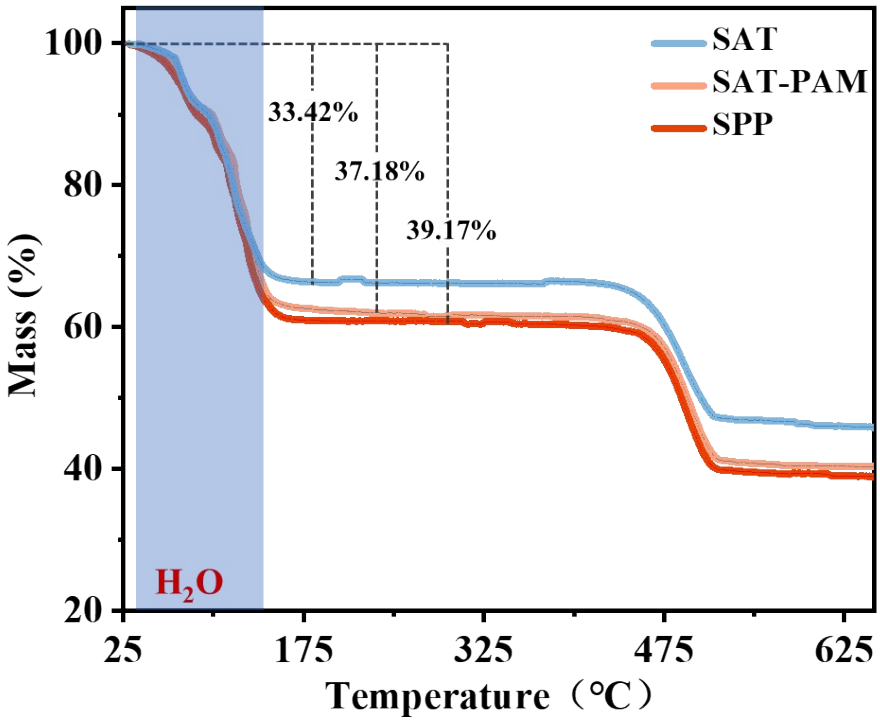

Figure S7 TGA curves of SAT, SAT-PAM and SPP composites.

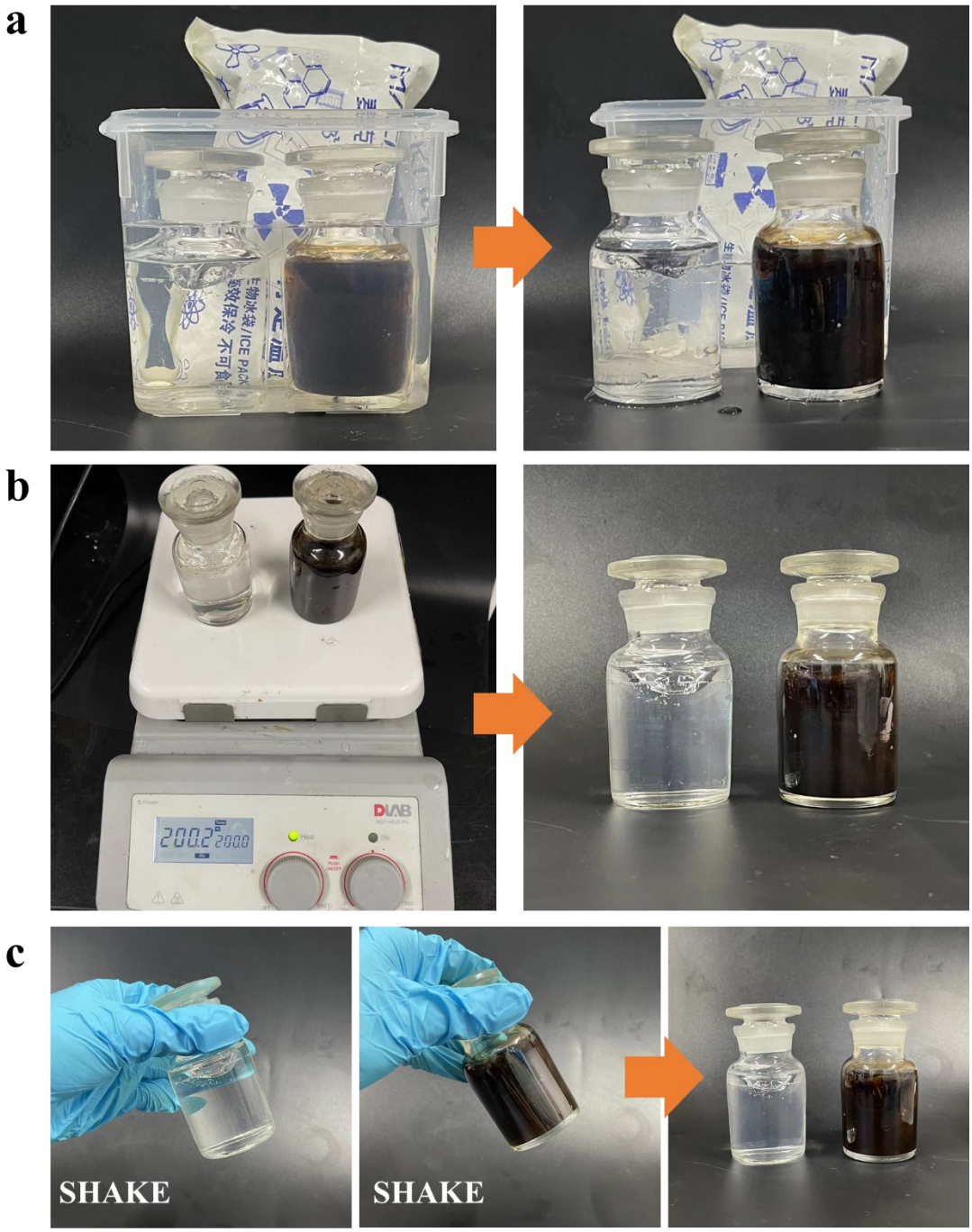

Figure S8 Photographs showing stable supercooling of SAT-PAM and SPP composites under different conditions: (a) cooling with ice bags, (b) heating on a hot plate followed by natural cooling, (c) undergoing violent shaking.

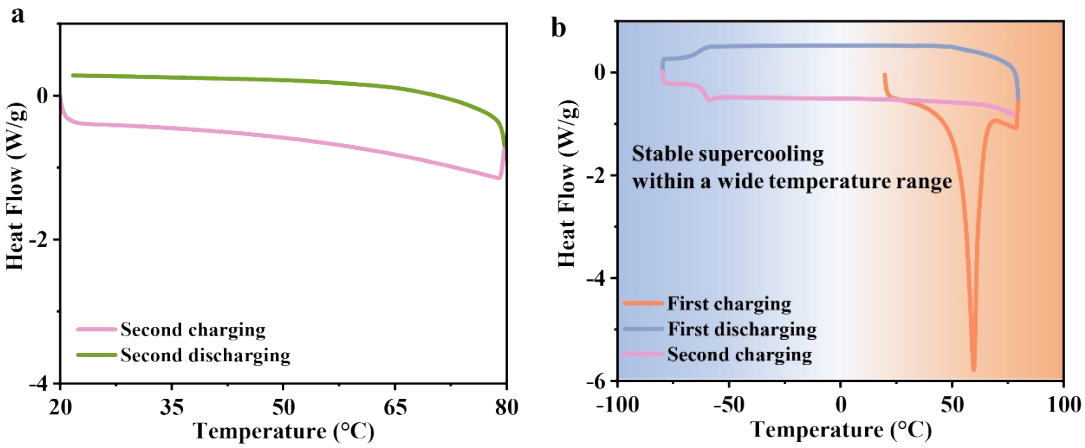

Figure S9 (a) DSC curve of supercooled SPP composite undergoing the second heating/cooling cycle; (b) DSC curves of SPP composite measured within a broad range of temperature from -80 °C to 80 °C.

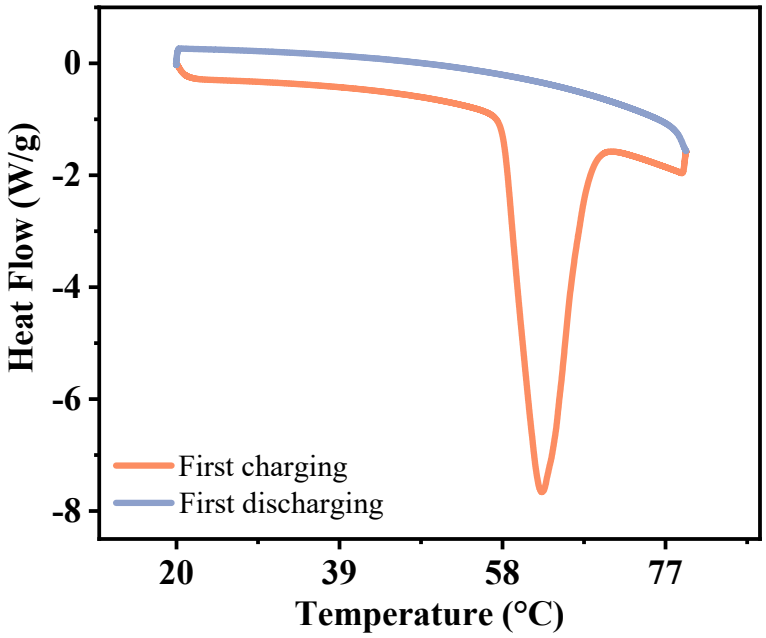

Figure S10 DSC curves of SAT during melting and cooling process.

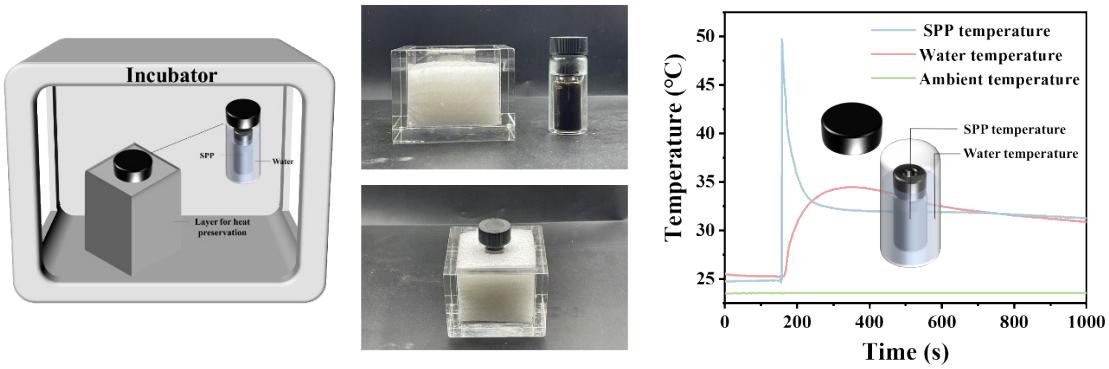

Figure S11 Schematic setup and photographs showing measurement of cold crystallization enthalpy of SPP composites.

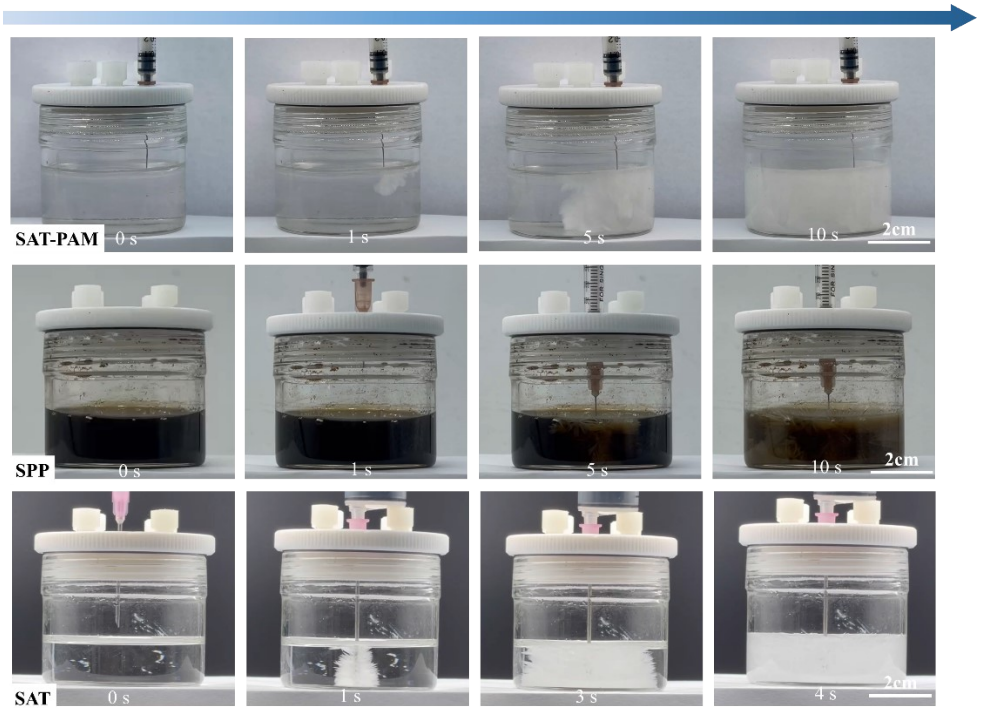

Figure S12 Time-sequential photos showing triggering crystallization of supercooled SAT-PAM, SPP and SAT through injecting SAT seed crystals. The hydrogel networks modulate the avalanche-like crystal growth behavior and enable controlled release of latent heat from supercooled SAT-PAM and SPP composites.

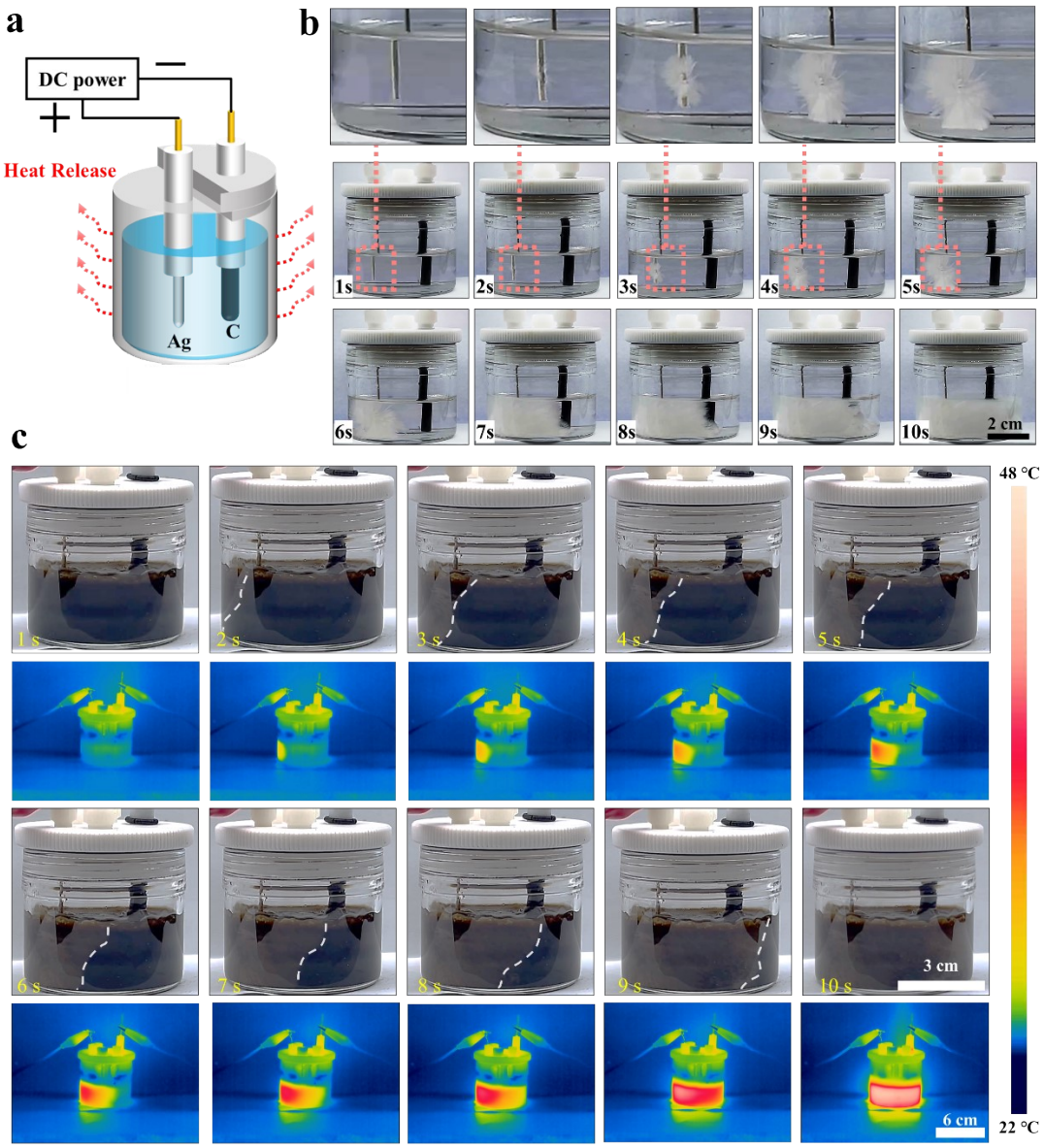

Figure S13 (a) Schematic setup for controlled release of stored latent heat through electrically triggering cold crystallization of supercooled hydrated salt composites. (b) Time-sequential photographs showing electrically-triggered crystallization of SAT-PAM composites. (c) Time-sequential photographs and infrared images showing electrically-triggered crystallization of SPP composites.

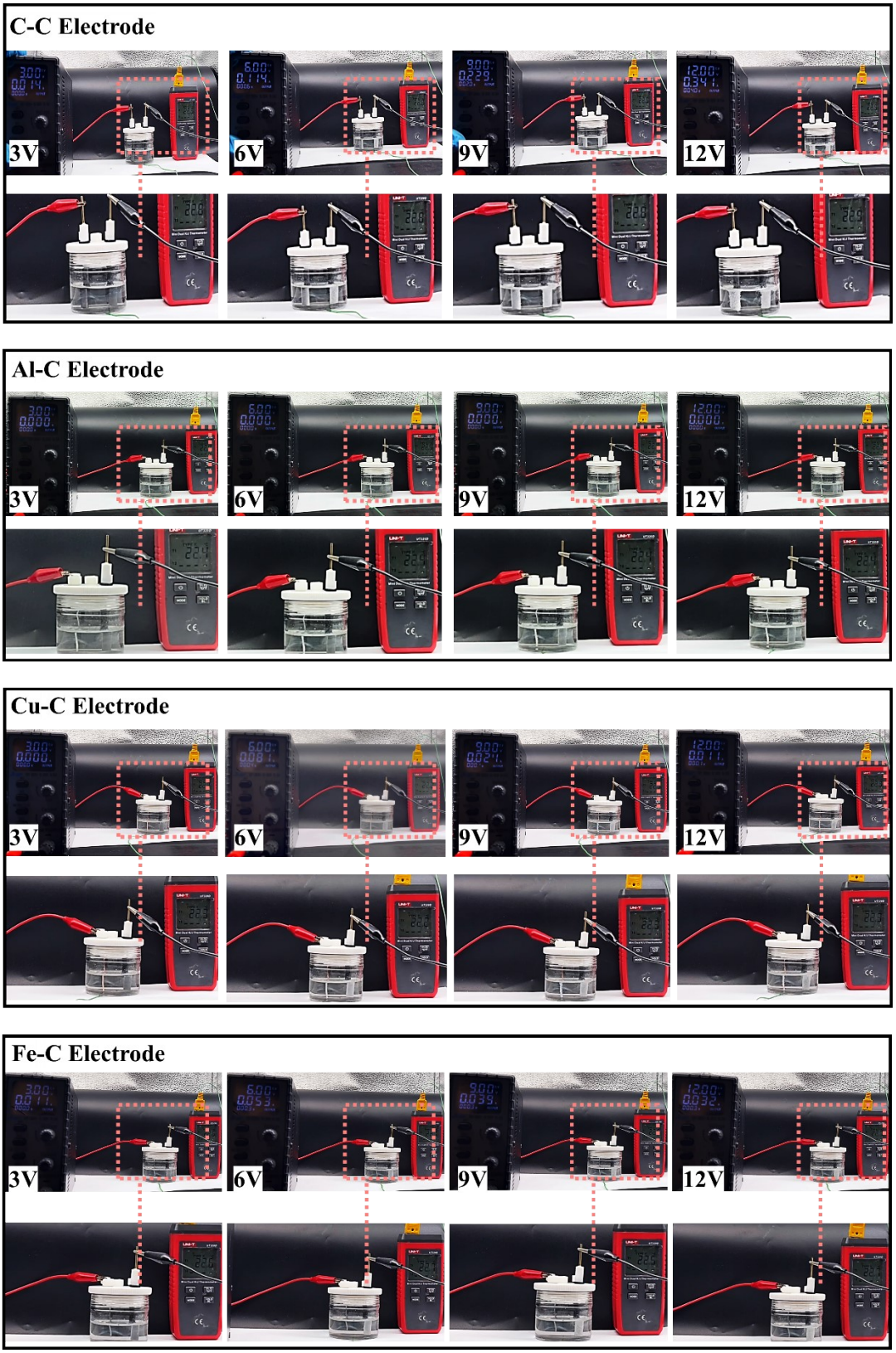

Figure S14 Photographs showing other paired electrodes failed to trigger crystallization of supercooled SAT composites.

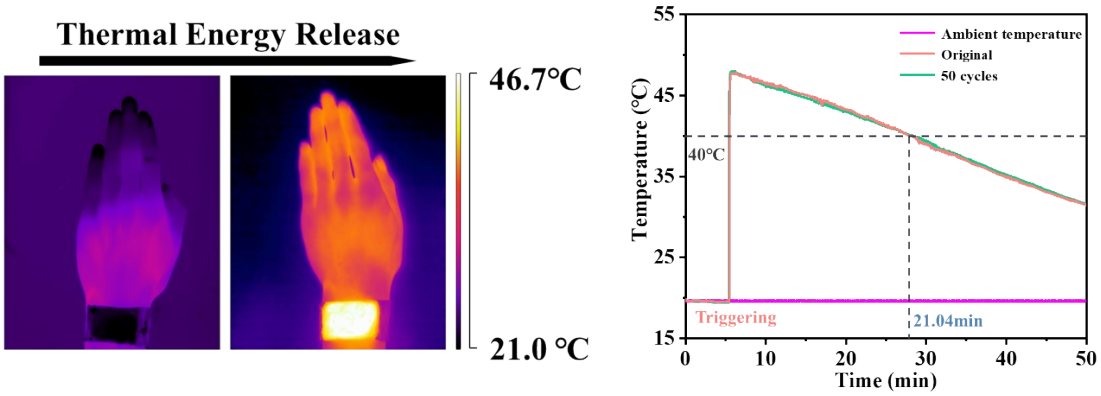

Figure S15 Controlled release of latent heat stored within supercooled SPP composites for thermotherapy applications: infrared images showing wearable composites for warming up human hand (left) and temperature evolution profiles of human wrist during thermotherapy (right).

Table S1 Summary of crystallization behavior of supercooled SPP composites triggered by applying electrical pulses

Voltage (DC)	Anode	Cathode	Electrode distances (mm)	Crystalline Position	Triggering response
3 V	Ag	Carbon	1, 2, 3	Anode	Success
6 V	Ag	Carbon	1, 2, 3	Anode	Success
9 V	Ag	Carbon	1, 2, 3	Anode	Success
12 V	Ag	Carbon	1, 2, 3	Anode	Success
3 V	Ag	Ag	1, 2, 3	Anode	Success
3 V	Ag	Cu	1, 2, 3	Anode	Success
3 V	Ag	Ti	1, 2, 3	Anode	Success
3 V	Cu	Carbon	1, 2, 3	——	No nucleation
6 V	Cu	Carbon	1, 2, 3	——	No nucleation
9 V	Cu	Carbon	1, 2, 3	——	No nucleation
12 V	Cu	Carbon	1, 2, 3	——	No nucleation
12 V	Cu	Cu	1, 2, 3	——	No nucleation
3 V	Al	Carbon	1, 2, 3	——	No nucleation
6 V	Al	Carbon	1, 2, 3	——	No nucleation
9 V	Al	Carbon	1, 2, 3	——	No nucleation
12 V	Al	Carbon	1, 2, 3	——	No nucleation
3 V	W	Carbon	1, 2, 3	——	No nucleation
6 V	W	Carbon	1, 2, 3	——	No nucleation
9 V	W	Carbon	1, 2, 3	——	No nucleation
12 V	W	Carbon	1, 2, 3	——	No nucleation